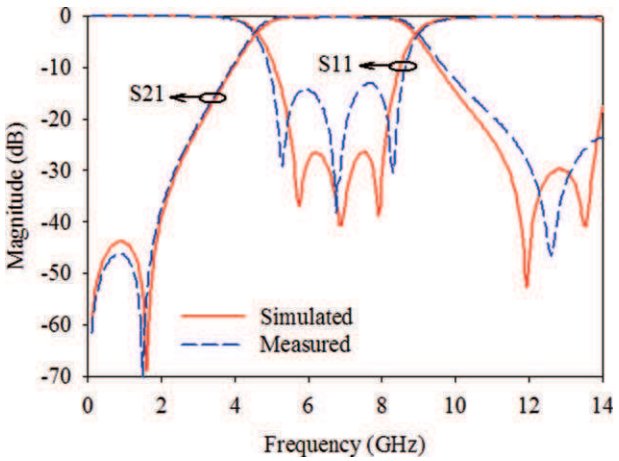

Figure 6 EM-simulated and measured performances of the proposed UWB coupled lines filter. [Color figure can be viewed in the online issue, which is available at wileyonlinelibrary.com]

filter occupies a small size of 8.7 mm by 2.4 mm. For the measurement, a 5-mm long microstrip feed line is added at both input and output. Figure 6 demonstrates the EM-simulated and experimental results of the proposed filter, where excellent agreement is obtained. The measured insertion loss is found to be less than 0.8 dB at the center frequency of the UWB passband. The measured return loss is better than 13 dB over the whole UWB passband. The filter shows the two new transmission zeros at the lower and upper edges of the desired passband, which enhanced the selectivity of the lower and the upper skirts of the UWB passband.

4. CONCLUSIONS

A compact UWB BPF using new microstrip parallel-coupled line structure has been developed and proposed in this letter. The filter has been constructed of only two sections of three-coupled lines, which is a quarter wavelength long at the mid-band frequency. To allow the filter to exhibit exhibits two new symmetric transmission zeros around the UWB passband, one of the outer coupled lines of each section was shorted to the ground. As a result, the two new transmission zeros around the passband enhanced the selectivity of both edges of the UWB passband significantly. The transmission zeros can be located at the desired frequency by adjusting the width or the length of the coupled lines or also by changing the gap between them. The desired bandwidth can be obtained where the bandwidth is reversely proportional to the gap between the coupled lines. The design is successfully realized and verified by full-wave EM simulation and the experiment. A good agreement between the expected and measured results is obtained and it validates the efficiency of the proposed new coupled line structure and corresponding filter design technique.

REFERENCES

1. FCC, Revision of Part 15 of the Commission's rules regarding ultra-wide-band transmission system, first note and order Federal Communication Commission, ET-Docket 98–153, 2002.
2. G.L. Matthaei, L. Young, and E.M.T. Jones, Microwave filters, impedance-matching network, and coupling structures, Artech House, Norwood, MA, 1980.
3. R. Schwindt and C. Nguyen, Spectral domain analysis of three symmetric coupled lines and application to a new bandpass filter, IEEE Trans MTT 42 (1994), 1183–1189.
4. J.-T. Kuo, E. Shih, and W.-C. Lee, Design of bandpass filters with parallel three-line coupled microstrips, in APMC2001 Proceedings, Taiwan, June 2001, pp. 157–160.
5. C. Nguyen, New compact wideband bandpass filter using three parallel-coupled lines, IEE Electron Lett 30 (1994), 2149–2150.
6. L. Zhu, S. Sun, and W. Menzel, Ultra-wideband (UWB) bandpass filters using multiple-mode resonator, IEEE Microwave Wirel Compon Lett 15 (2005), 796–798.
7. S. Sun and L. Zhu, Capacitive-ended interdigital coupled lines for UWB bandpass filters with improved out-of-band performance, IEEE Microwave Wirel Compon Lett 16 (2006), 440–442.
8. Y.-C. Chiou, J.-T. Kuo, and E. Cheng, Broadband quasi-Chebyshev bandpass filters with multimode stepped- impedance resonators (SIRs), IEEE Trans Microwave Theory Tech 54 (2006), 3352–3358.
9. S. Wong and L. Zhu, Quadruple-mode UWB bandpass filter with improved out-of-band rejection, IEEE Microwave Wirel Compon Lett 19 (2009), 152–154.
10. H. Shaman and J.S. Hong, Asymmetric parallel-coupled lines for notch implementation in UWB filter, IEEE Microwave Wirel Compon Lett 17 (2007), 516–518.
11. Sonnet Software Inc., EM User's manual, Ver. 12, Sonnet Software Inc., NY, 2005.

A TRIPLE-BAND WLAN/WiMAX PRINTED MONOPOLE ANTENNA FOR MIMO APPLICATIONS

Ali Foudazi, Alireza Mallahzadeh, and Sajad Mohammad Ali Nezhad
Department of Electrical and Electronic Engineering, Shahed University, Tehran, Iran; Corresponding author: alinezhad@shahed.ac.ir

Received 30 July 2011

ABSTRACT: *A triple-band multi-input multi-output (MIMO) antenna is presented. The proposed antenna consists of a C-shaped monopole antenna that provides dual-band resonant antenna. By protruding an L-shaped parasitic strip on the ground plane, a third band as well as enhancement of the isolation between two ports in MIMO array is achieved. The proposed antenna can cover 2.1–2.6, 3.3–4, and 5.4–6 GHz, which are allocated for WLAN and WiMAX applications. The proposed triple-band antenna structure is used in different two-element MIMO arrays. Simulation results show that the S_{11}, S_{12}, and S_{22} of the MIMO arrays are independent of the position of the two-element. The results show good S-parameters, high peak gain and radiation efficiency, and stable radiation patterns among the triple-band coverage.*

Microwave Opt Technol Lett 54:1321–1325, 2012; View this article online at wileyonlinelibrary.com.
DOI 10.1002/mop.26799

Key words: *monopole antenna; MIMO system*

1. INTRODUCTION

Multi-input multi-output (MIMO) systems that utilize multiple antennas to increase channel capacity without sacrificing additional spectrum or transmitted power have received a great deal of attention recently. In modern wireless communication systems, high data rate is required over band limited channels. MIMO antenna should provide high radiation efficiency, low envelope correlation, and high isolation between the signal ports. To achieve maximum channel capacity, the array is also required having a high gain and wide lobe pattern [1]. To obtain an antenna, which can be used for MIMO applications, different

shapes of printed antenna are reported in the literature. Several triple-band MIMO antennas are given in Refs. 1–3. In Ref. 1, it is shown that different MIMO arrays provide high peak gain, good envelope correlation and good *S*-parameters among three bands. However, this structure is unable to cover 3.5 GHz for WiMAX. In Ref. 2, the MIMO array can only be used in orthogonal configuration to provide suitable *S*-parameters. Also, a planar triple-band MIMO array with invert-F structure is presented in Ref. 3 for 2.4/5.2/5.8 GHz bands. A MIMO antenna with two sets of printed radiators and slits on the ground plane operating at 2.4 GHZ for WLAN application is presented in Ref. 4. In Ref. 5, a dual-band printed diversity antenna for UMTS (2000 MHz) and WLAN (2400 MHz) is presented.

The design of modern communication systems demand multiband antenna which can cover both WLAN and WiMAX for a single system. Different studies focused on the design of printed antennas which operate at WLAN and WiMAX frequency bands. A monopole antenna with branch slit is given in Ref. 6 and covers 2.3–2.9, 3.1–4, and 4.9–6 GHz which fits the requirement of WiMAX operation antenna. The antenna covers 2.4, 3.5, and 5 GHz. A dual-wideband antenna for WLAN/WiMAX application is given in Ref. 7, which covers 2.4/5.2/5.8 GHz (WLAN) and 2.5/3.5/5.5 GHz (WiMAX). A very small-sized penta-band hand-shaped monopole antenna for 2.4/3.3/3.7/5.2/5.8 GHz is presented in Ref. 8 for WLAN and WiMAX application.

In this article, a printed triple-band antenna is presented for 2.4/5.8 GHz WLAN and 2.5-/3.3-/3.5-/3.7-/5.5-GHz WiMAX. A C-shaped monopole patch is provided with dual-band behavior. By protruding an additional L-shaped strip above the ground plane, the third band is achieved. The *S*-parameters of two-element arrays of the proposed antenna in different configurations are investigated, and the results of the pair that provides the best *S*-parameters, radiation patterns, mutual coupling and envelope correlation are given. All the simulations are carried out using the commercially available software package HFSS.

2. MULTIBAND ANTENNA DESIGN

It is known that the C-shaped monopole antenna can provide dual-band behavior due to two resonance paths [9]. By changing the lengths of the two different paths, the center frequencies of dual-band operation can be tuned. The top view of the dual-band antenna is shown in Figure 1(a). The substrate of the antenna is 18×40 mm^2 and prototyped on FR4 which is $\varepsilon_r = 4.4$, $\tan \delta = 0.02$, and $h = 1$ mm. The dual-band radiator is excited by a microstrip-fed line. The width of the fed line is 1.86 cm to achieve 50-Ω characteristic impedance. At the bottom side of the substrate, a rectangular plane is used as a ground plane. The bottom view of the dual-band antenna is presented in Figure 1(b). The length of the ground plane is 8 cm. By using an additional protrudent open-circuit strip that is shown in Figure 1(c), a triple-band monopole antenna is achieved. The proposed antenna covers 2.1–2.6, 3.3–4, and 5.4–6.1 GHz that corresponds to 2.4-/5.8-GHz WLAN and 2.5-/3.3-/3.5-/3.7-/5.5-GHz WiMAX, respectively. Figure 2 shows the S_{11} of the proposed antenna with and without the L-shaped protrudent strip on the ground plane. It is obvious that the L-shaped path is mostly responsible for 3.3–4 GHz.

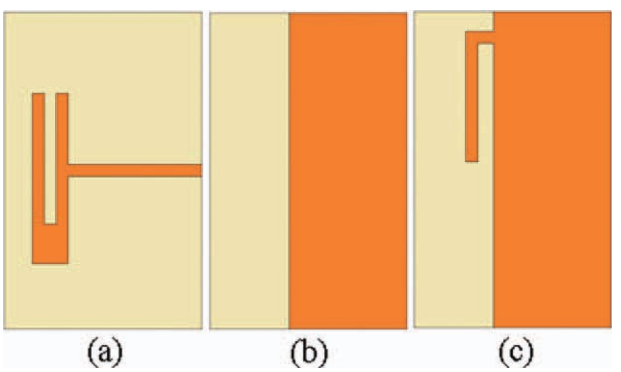

Figure 1 Propose multiple-band antenna, (a) C-shaped radiator, (b) simple rectangular ground plane, and (c) ground plane with additional L-shaped strip. [Color figure can be viewed in the online issue, which is available at wileyonlinelibrary.com]

3. MIMO DESIGN

The triple-band antenna is considered for 2.1–2.6, 3.3–4, and 5.4–6.1 GHz for WLAN/WiMAX application. This antenna element can be arranged in different ways for use in MIMO applications. The performance of an antenna array suitable for MIMO systems depends on various parameters such as *S*-parameters, envelope correlation, peak gain and stable radiation patterns. Seven possible configurations that any two such monopole antennas can be arranged in beside each other are presented in Figure 3. The spacing between different array elements is obtained by choosing the lowest space between two radiators. The substrate dimension of the Figures 3(a)–3(c) are 18×80 mm^2. Also in this figure, the minimum possible spacing between two radiators is 20.5, 16.5, and 6.5 mm respectively. The substrate dimension of the Figures 3(d)–3(f) are 24×72 mm^2. Also in this figure, the minimum possible spacing between two radiators is 8.5, 10.5 and 12.5 mm, respectively. The substrate dimension of the Figures 3(g)–3(h) are 39.5×55.5 mm^2. Also in this figure, the minimum possible spacing between two radiators is 11.25. The relevant simulated *S*-parameters of the MIMO arrays are given in Figure 4. It is obvious that by using a protrudent L-shaped strip on the ground plane, S_{11} and S_{22} of the two elements in various configurations of MIMO array have not changed from the single triple-band antenna. Different array configurations show changes in mutual coupling of the antenna. It is also seen that the various parallel configurations of the two-element arrays have good results, while in Refs. 1 and 2 the orthogonal configuration provides only low mutual coupling in MIMO arrays. From Figure 4, it can be seen that the horizontally flipped two-element of the array structure seen in Figure 3(a) has mutual coupling of less than 20 dB. The configuration of Figure 3(a) is fabricated on FR4 with 1 mm thickness. The measured *S*-parameters of the proposed prototype MIMO array

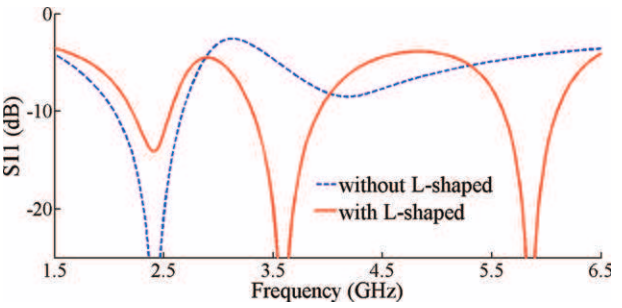

Figure 2 Simulated S_{11} of the proposed antenna with and without L-shaped strip. [Color figure can be viewed in the online issue, which is available at wileyonlinelibrary.com]

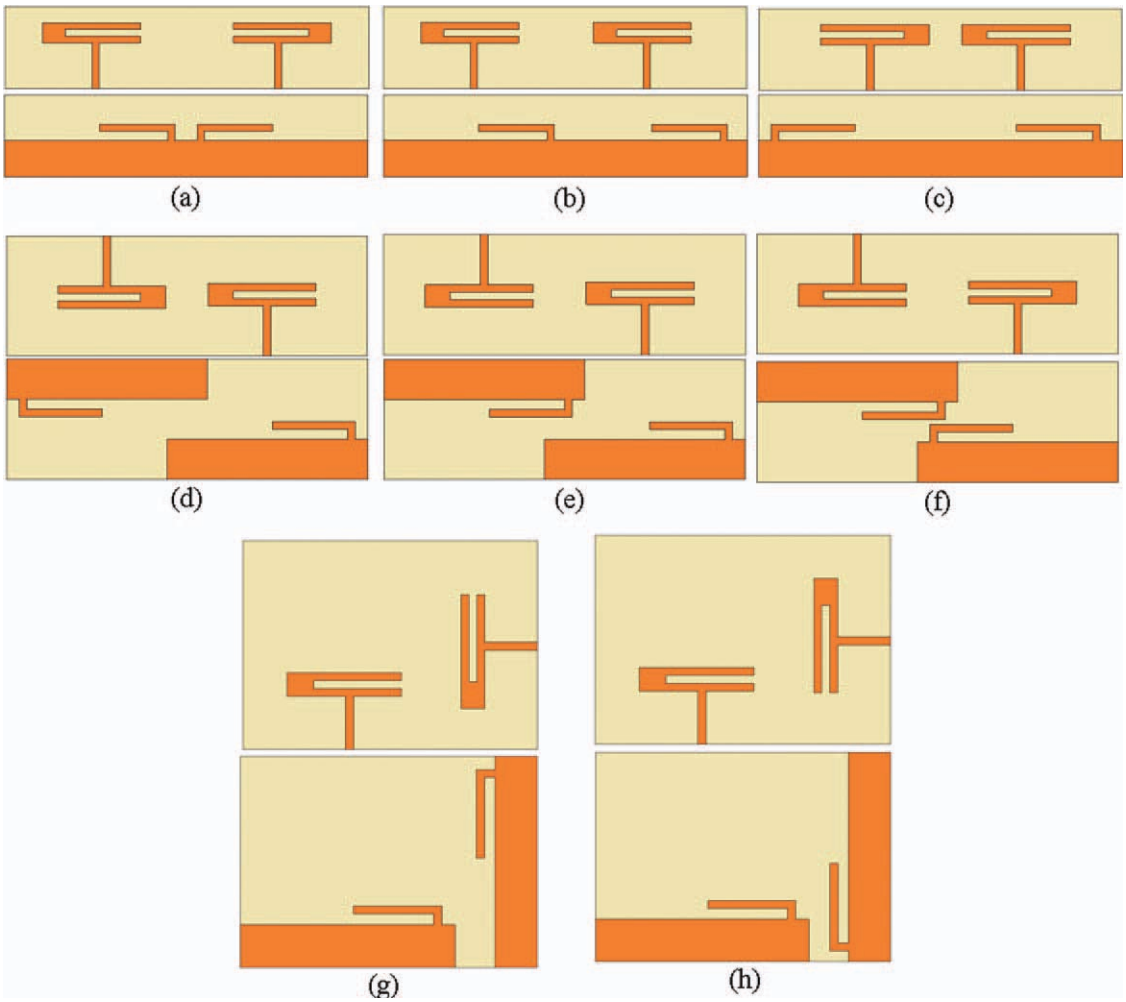

Figure 3 Different MIMO configurations of the propose triple-band antenna. [Color figure can be viewed in the online issue, which is available at wileyonlinelibrary.com]

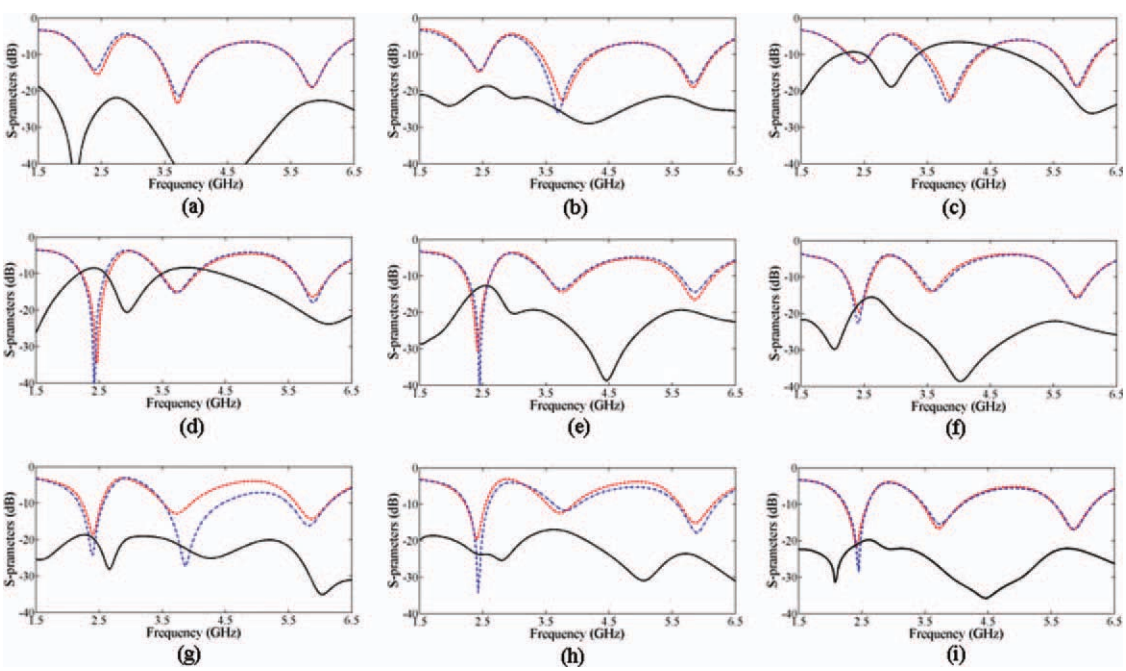

Figure 4 S-parameters of the proposed triple-band antenna in MIMO configurations (a)–(h) relevant to the Figure 5, (i) measured results of the proposed MIMO array of Figure 5(a). [Color figure can be viewed in the online issue, which is available at wileyonlinelibrary.com]

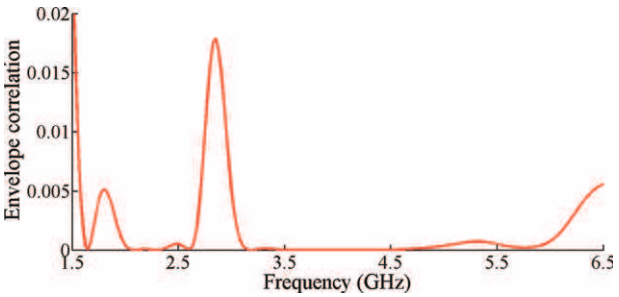

Figure 5 Measured envelope correlation of the proposed triple-band MIMO antenna. [Color figure can be viewed in the online issue, which is available at wileyonlinelibrary.com]

are presented in Figure 4(i) and shows good agreement with those of the simulation.

4. RESULTS AND DISCUSSION

To confirm the quality of the proposed triple-band antenna for MIMO applications, several parameters should be given. The envelope correlation of a MIMO array antenna can be computed from the *S*-parameters by using the following formula [1]:

$$\rho_e = \frac{|S_{11} * S_{21} + S_{12} * S_{22}|^2}{\left|\left(1 - |S_{11}|^2 - |S_{21}|^2\right)\left(1 - |S_{22}|^2 - |S_{12}|^2\right)\right|}$$

Figure 5 shows the measured envelope correlation of the proposed MIMO array. The value of the envelope correlation is less than 0.005, which is practically acceptable. The measured radiation efficiency of the proposed MIMO array among the triple-band for WLAN/WiMAX application is given in Table 1. From the results, it can be seen that radiation efficiency of the proposed MIMO array is always greater than or equal to 90%. The radiation patterns of the proposed MIMO array at 2.4, 3.5, and 5.8 GHz are given in Figure 6. It is clear that the WLAN/WiMAX MIMO antenna has stable radiation patterns in both principal planes. The proposed triple-band MIMO antenna is constructed and shown in Figure 7.

The low mutual coupling, good impedance matching, low envelope correlation, high radiation efficiency and stable radiation patterns in both principal planes confirm that the proposed MIMO array is a good candidate for use in WLAN/WiMAX MIMO systems.

5. CONCLUSIONS

A triple-band printed monopole antenna for WLAN/WiMAX application is presented. The proposed antenna covers 2.4-/5.8-GHz WLAN and 2.5-/3.3-/3.5-/3.7-/5.5-GHz WiMAX. Different types of two-element MIMO arrays of the triple-band antenna are simulated. The proposed construction of the vertically flipped MIMO array of the triple-band antenna provides several features desirable for MIMO systems, such as low mutual coupling, good impedance matching, low envelope correlation, appropriate peak gain, high radiation efficiency and good radiation patterns; features which are desired for MIMO systems.

TABLE 1 Measured Radiation Efficiency of the Proposed MIMO Array

Frequency (GHz)	2.4	3.7	5.8
Radiation efficiency	92%	94%	90%

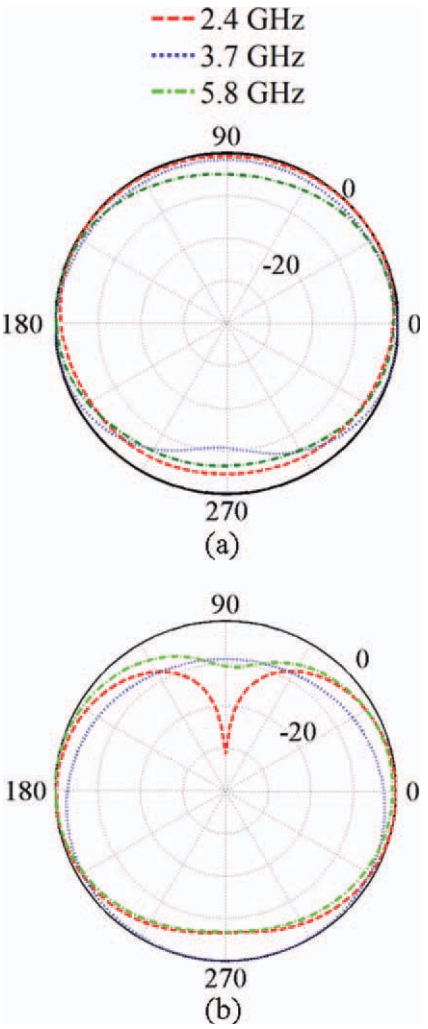

Figure 6 Measured radiation patterns of the proposed triple-band MIMO antenna (a) *H*-plane, (b) *E*-plane. [Color figure can be viewed in the online issue, which is available at wileyonlinelibrary.com]

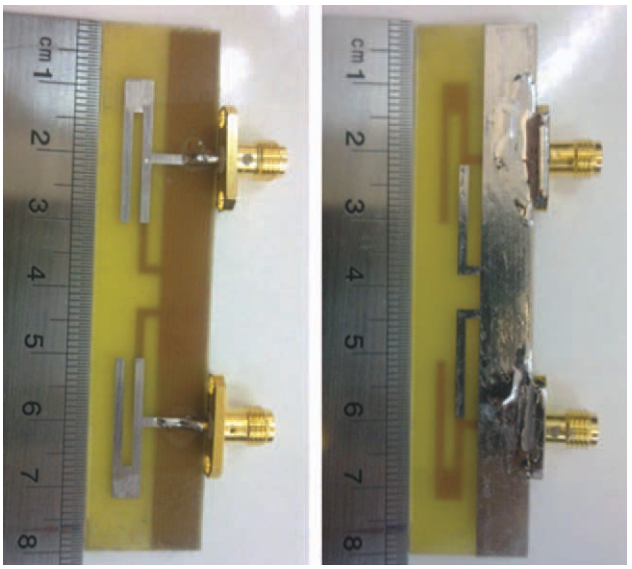

Figure 7 Constructed triple-band MIMO antenna. [Color figure can be viewed in the online issue, which is available at wileyonlinelibrary.com]

Also, it is shown that the measured results correlate well with simulations.

REFERENCES

1. S.M.A. Nezhad and H.R. Hassani, A novel triband E-shaped printed monopole antenna for MIMO application, IEEE Antennas Wirel Propag Lett 9 (2010), 576–579.
2. A. Mallahzadeh, A. Sedghara, and S.M.A. Nezhad, A tunable multi-band meander line printed monopole antenna for MIMO systems, Proceedings of the 5th European Conference on Antenna and Propagation (2010), 315–318.
3. D.W. Browne, M. Manteghi, M. Fitz, and Y. Rahmat-samii, Experiments with compact antenna arrays for MIMO radio communications, IEEE Trans Antennas Propag 54 (2006), 3239–3250.
4. H. Li, J. Xiong, and S. He, A compact planar MIMO antenna system of four elements with similar radiation characteristics and isolation structure, IEEE Antennas Wirel Propag Lett 8 (2009), 1107–1110.
5. Y. Ding, Z. Du, K. Gong, and Z. Feng, A novel dual-band printed diversity antenna for mobile terminals, IEEE Trans Antennas Propag 55 (2007), 2088–2096.
6. W.-S. Chen and Y.-C. Cheng CPW-fed printed monopole antenna with branch slits for wimax applications, Microwave Opt Technol Lett 50 (2008).
7. L.-H. Ye and Q.-X. Chu, Compact dual-wideband antenna for WLAN/WIMAX applications, Microwave Opt Technol Lett 52 (2010).
8. A. Mallahzadeh, A. Foudazi, and S.M.A. Nezhad, A small-size pentaband hand-shaped coplanar waveguide-fed monopole antenna, Microwave Opt Technol Lett 53 (2011).
9. C.-Y. Huang and P.-Y. Chiu, Dual-band monopole antenna with shorted parasitic element, Electron Lett 41 (2005).

EFFICIENT MINIATURIZATION TECHNIQUE FOR WIRE PATCH ANTENNAS

Rafik Addaci, Aliou Diallo, Philippe Le Thuc, and Robert Staraj
Laboratoire d'Electronique, Antennes et Télécommunications
Université de Nice-Sophia Antipolis, CNRS-UMR 6071 Bât. 4, 250 rue A. Einstein, 06560 Valbonne, France; Corresponding author: rafik.addaci@unice.fr

Received 14 July 2011

ABSTRACT: *In this article, a new miniaturization technique for a circular wire patch antenna is presented. This technique consists in adding cylindrical skirts to the two metallic circular plates. A parametric study carried out for this new design shows that this new shape gives one more degree of freedom to control the resonance frequency and allows us to optimize the matching of this smaller radiating element in the desired operation band.* © 2012 Wiley Periodicals, Inc. Microwave Opt Technol Lett 54:1325–1327, 2012; View this article online at wileyonlinelibrary.com. DOI 10.1002/mop.26761

Key words: *antenna miniaturization techniques; monopolar radiation pattern; wire patch antenna; Zigbee standard*

1. INTRODUCTION

For several years, one of the main challenges in the antennas technology is focused on the reducing of their global dimensions, which are often too important independently of the application. In this kind of research, it has been shown that a microstrip antenna can be used below its well-known classical fundamental mode by including ground wires connecting the patch antenna to the ground plane [1] [2]. Because of their low-profile, large bandwidth and monopolar type radiation pattern, wire patch antennas are interesting but their ground planes are generally too cumbersome compared with the size of the radiating element. The structure presented in this article has the advantage to work with a very small ground plane, concurrently with the properties of the antenna described in Refs. 1 and 2 and has smaller dimensions. The methodology proposed to achieve a miniaturized wire patch antenna is applied for Zigbee wireless applications [3], because its geometry is also very suitable to the integration of the RF electronic stage under the natural protection created by the ground plane and the skirt.

2. ANTENNA DESIGN AND WORKING PRINCIPLE

Figure 1 presents the initial antenna geometry [4]. The structure is made up of two circular metallic plates realised in 0.3-mm copper sheets on air substrate to provide the largest bandwidth. The upper plate, which is considered as the radiating element, is center fed by a coaxial probe. Two ground wires connect this upper plate to the ground plane. The addition of these shorting wires connecting the upper patch to the lower one (considered as the ground plane of these kind of antennas) is the particularity of wire patch antennas [1, 2, 5]. These shorting pins, located symmetrically on each side of the coaxial probe feed, can be considered as equivalent inductances set in parallel with the patch ***capacitance's, which create a parallel resonance located below the well-known classical fundamental mode of the antenna. Our purpose is here to design a smaller low profile circular wire patch antenna dedicated to 2.4–2.5-GHz Zigbee application. Several solutions exist to reduce the size of this kind of antennas [6, 7] using however stacked patches to keep a very large bandwidth. Our goal is to find an efficient miniaturization technique to reduce the dimensions of the initial circular wire patch antenna (Fig. 1) to obtain a new smaller antenna having the same performance. However, by reducing the size of any antenna, it is well known that a shift to higher frequencies is generally obtained. To reduce the dimensions of these kind of antennas without changing their operation frequency, our technique consists in increasing vertically the size of the upper patch by bending the metallic plate to form a cylindrical skirt. After a first parametric study, we have observed that for some considered dimensions, it was not possible with this new parameter to place the resonance frequency in the desired band. Furthermore for some cases, the adaptation level was not sufficient for our application. That is why the same technique was also applied to the ground plane, allowing to obtain a new freedom degree which makes possible a better control of the performance of this antenna in terms of resonance frequency and adaptation level and reduces its overall dimensions (Fig. 2).

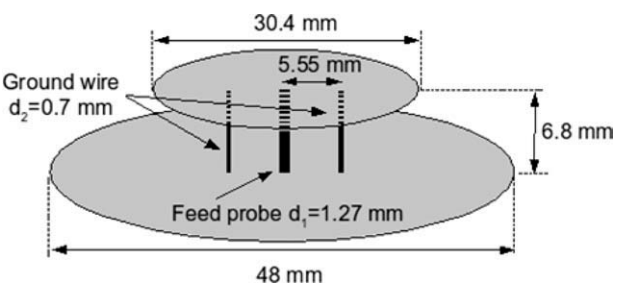

Figure 1 Initial antenna geometry